draft version

Evolution of cross-correlation and time lag of 4U 1735-44 along the branches

Ya-Juan Lei[1], Hao-Tong Zhang[1], Cheng-Min Zhang[1],Jin-Lu Qu[2], Hai-Long Yuan[1], Yi-Qiao Dong[1], Yong-Heng Zhao[1],De-Hua Wang[3], Hong-Xing Yin[4], Li-Ming Song[2]

ABSTRACT

We analyze the cross-correlation function between the soft and hard X-rays of atoll source 4U 1735-44 with *RXTE* data, and find the anti-correlated soft and hard time lags of about hecto-second. On the island state, the observations do not show any obvious correlations, and most observations of banana branch show positive correlation. However, the anti-correlations are detected on the upper banana branch. These results are different from those of Z sources (Cyg X-2, GX 5-1), where the anti-correlation is detected in the low luminosity states, then the lag timescales of both this atoll and Z sources are found to be similar, at the magnitude of several tens to hundreds of seconds. As a comparison, it is noted that the anti-correlated lags of thousand-second have been reported from the several black hole candidates in their intermediate states. Finally, we compare the correspondent results of atoll source 4U 1735-44 with those observed in black hole candidates and Z sources, and the possible origins of the anti-correlated time lags are discussed.

Subject headings: accretion, accretion disk–binaries: close–stars: individual (4U 1735-44)–X-rays: binaries

[1]Key Laboratory of Optical Astronomy, National Astronomical Observatories, Chinese Academy of Sciences, Beijing 100012, P.R. China; leiyjcwmy@163.com

[2]Particle Astrophysics Center, Institute of High Energy Physics, Chinese Academy of Sciences, Beijing 100049, P.R. China

[3]Astronomy Department, Beijing Normal University, Beijing 100875, P.R. China

[4]School of Space Science and Physics, Shandong University, Weihai, 264209, P.R. China

1. Introduction

The timing and spectral analysis of the X-ray emission of the compact objects, neutron stars (NSs) or black holes (BHs), can exhibit the accreting flow properties of low-mass X-ray binaries (LMXBs) (see, e.g., van der Klis 2006; Liu et al. 2007a). Based on the X-ray spectral properties, which are shown in the defined color-color diagram (CCD) or hardness-intensity diagram (HID), the NS LMXBs can be classified into two subtypes, Z sources with high luminosity and atoll sources with low luminosity (Hasinger & van der Klis 1989). The main difference between atoll and Z sources might be the accretion rate and magnetic field, where Z source shares the higher accretion rate and slightly stronger magnetic field than those of atoll source (Zhang 2007). The atoll sources cover a wider range of luminosity, whereas Z sources usually appear as the Eddington limited luminosities (e.g., Ford et al. 2000). Z (atoll) source traces out a Z-shape track (island + banana pattern) within a few days (days to weeks). In CCD, the Z-track consists of three main branches, horizontal branch (HB), normal branch (NB) and flaring branch (FB) (Hasinger & van der Klis 1989; Hasinger 1990). The source evolves continuously along the Z-track, with each position related to the different mass accretion rate. The accretion rate increases from HB to NB and reaches a maximum at the right end of the FB (Hasinger et al. 1990). However, recently, the results of studying the source XTE J1701-462 suggest that the motion along the Z branches might be corresponding to the roughly constant accretion rate (Lin et al. 2009; Homan et al. 2010).

As for the CCD pattern of atoll source, it follows the similar correspondences to those of Z source, from island state (IS) to the lower left banana (LLB), lower banana (LB) and upper banana (UB) (van der Klis 2000; Altamirano et al. 2008). In the atoll source, the count rates increase with the inferred accretion rate $\dot{M}$, which increases from the IS to the UB. Some atoll sources show the Quasi-periodic oscillations (QPOs) in the LLB (van der Klis 2000, 2006; Belloni et al. 2007). QPOs are usually not detected in the IS, which may be on account of the low sensitivity at the low count rates.

The spectral characteristics of Black hole X-ray binaries (BHXBs) usually exhibit five distinct states, quiescent state, low/hard state(LHS), intermediate state (IMS), high/soft state (HSS), and very high state (VHS) (Remillard 2005; Remillard & McClintock 2006; Belloni 2010). The IMS is complex, whose luminosity could not be determined solely by the mass accretion rate (Yu & Dolence 2007; Yu & Yan 2009). Although the luminosity of VHS is much higher than that of IMS, both states share the similar spectral and timing behaviors, which can be taken as the same state that represents the transitions between LHS and HSS (Done et al. 2007).

The timing properties of X-ray binary are related to the spectral states i.e., the positions of CCD. The cross-correlation function of the soft and hard X-ray photons can be used for

analyzing the relation of different energy bands, which is helpful for understanding the radiative and geometrical structure of the accretion disk for different spectral states. The cross-correlated soft and hard X-ray lags have been investigated for Z sources and BHXBs. For some BHXBs, the anti-correlation of a few hundred seconds are often seen in the steep power-law (SPL) or intermediate states (Choudhury et al. 2005; Sriram et al. 2007, 2009, 2010), and these timescales of the lags could be ascribed to the viscous timescales of matter flows in the optically thick accretion disks (Choudhury & Rao 2004). Such anti-correlated lags ($\sim$ several 10-100 s) are also detected on the HB and upper NB of two Z sources (Cyg X-2, GX 5-1) (Lei et al. 2008; Sriram et al. 2012). The simulation by Sriram et al. (2010) indicates that the phenomena of observed anti-correlations should not arise from the spurious nature, but the reality of physical processes.

In some aspects, the atoll source and BH system share the similar spectral characteristics (di Salvo et al. 2006), thus we select an atoll source, 4U 1735-44, to study its evolution of cross-correlation and time lag between the soft and hard X-rays. This source is classified as an atoll source with a relatively high luminosity (Smale et al. 1986; Seon et al. 1997), the distance of which is measured to be about 8.5 kpc (Galloway et al. 2008). The binary parameters of 4U 1735-44 have been observed with the orbital period of 4.654 hr (Corbet et al. 1986) and its companion mass of 0.53 ± 0.44 $M_{\odot}$ (Casares et al. 2006). Its X-ray spectra are analyzed by Ng et al. (2010) and Mueck et al. (2011), with an iron emission line detected. In addition, the kHz QPOs are discovered at the relatively lower mass accretion rates (Ford et al. 1998; Wijnands et al. 1998). In detail, we investigate whether the anti-correlation between the soft (2-3.3 keV) and hard (12-30 keV) X-rays exists in 4U 1735-44. As a further step, we compare the results of atoll with those of Z sources and BHXBs. The organization of the paper is described below. Section 2 is about the observations and data analysis of *RXTE*, and the results on the cross-correlation between the soft and hard X-rays are analyzed in section 3. The discussions and summary are written in section 4.

2. Observation and Data Reduction

We analyze all pointed observations of the Proportional Counter Array (PCA) on board the *RXTE* satellite. The PCA consists of 5 non-imaging, coaligned Xe multiwire proportional counter units (PCUs). In the work, only PCU2 data are adopted, which is the best calibrated unit and has the longest observational duration. After excluding the data segments less than 2000 s, we extract the light curves from the data of standard 2 mode with bin size of 16 s. With the XRONOS tool "*crosscor*", we estimate the coefficient of the cross-correlation between the soft (2-3.3 keV) and the hard (12-30 keV) X-rays.

Similar to the previous publication about the cross-correlation for Z source Cyg X-2, we divide the cross-correlation results into three groups, the positive, ambiguous and anti-correlated (also see Lei et al. 2008). We can obtain the time lag by fitting the anti-correlated part with an inverted Gaussian function. After subtracting the background, the light curves and anti-correlations between soft and hard X-rays, accompanying with the pivoting spectra from the data with different hardness ratios, are shown in Figure 1, where we define the hard and soft regions according to the hardness ratios.

In order to study the source evolution on the CCD of 4U 1735-44, we define the soft and the hard colors as the count-rate ratios 3.5-6.0 keV/2.0-3.5 keV and 9.7-16 keV/6.0-9.7 keV (also see O'Brien et al. 2004). The light curves are extracted from the 2.0-3.5 keV, 3.5-6.0 keV, 6.0-9.5 keV and 9.5-16 keV, respectively, with the background subtracted. By the corresponding Crab values, we correct the affections of the different gain epochs and the gain change (van Straaten et al. 2005). Figure 2 shows the revised CCDs with the bin size of 512 s. For spectral analysis, the PCA background subtraction is carried out using the latest versions of the appropriate background models, and a 0.6% systematic error is added to the spectra to account for the calibration uncertainties. As usual, the spectral fitting software *XSPEC* is used.

3. Results

3.1. The results of cross-correlations and their distribution on CCD

With the data of *RXTE*, for the atoll source 4U 1735-44, we analyze the cross-correlation between the soft (2-3.3 keV) and hard (12-30 keV) X-rays. For each segment of the light curves, we analyze the cross-correlation. The anti-correlations have been detected in the light curves of 12 observations. We apply the letter 'a' to mark the segment of the anti-correlation. The ranges of hard and soft time lags for the anti-correlation are from a few tens to hundred seconds. There are four regions in Figure 2 that shows the CCD of all analyzed observational data. The data in region 'I', 'II', 'III' and 'IV' are mainly related to the IS, LLB, LB and UB, respectively.

In Table 1, we list the observations with anti-correlation detected, the cross-correlation coefficients and delay times. From Table 1 and Figure 2, we notice that most of the anti-correlated observations are located at the UB, where show the 7 observations with anti-correlated hard X-ray lags, 3 observations with anti-correlated soft X-ray lags and 2 observations with unobvious time lag. The delay times are similar to those found in the Z sources Cyg X-2 and GX 5-1 (Lei et al. 2008; Sriram et al. 2012). There is no relation detected

between the delay times and the location in region 'IV' of Figure 2.

From Figure 2 and Table 2, we can see that, in the region 'I', ambiguous correlated data are dominated, then the great majority of positively correlated data dominate in the regions 'II' and 'III', and in the region 'IV', all the three correlations are found in the equal weight. Averagely, the correlation coefficients of the region 'II' are mostly less than those of region 'III'. Obviously, most anti-correlated data occur in regions 'IV'. In addition, for the observations with the anti-correlations, the spectral evolution of the soft and hard regions of the light curves is shown in Figure 1. However, the energy ranges of the pivoting are not obviously evolutional along the locations of the CCD. There is not yet found the pivoting in the spectral evolution of positive-correlation between the soft and hard X-rays, which is consistent with the results of Lei et al. (2008) and Sriram et al. (2012).

3.2. Spectral variation

It is known from the previous work that the position in the CCD generally is well correlated to its spectral/timing state (see, e.g., van der Klis 2006). For studying the spectral evolution during the positive and anti-correlation between soft and hard X-rays, we analyze the spectra of the segments a, b, c and d (account rates decrease from a to d) of ObsID 91025-01-04-03, separately. For segment a, the cross-correlation between soft and hard X-rays shows anti-correlation, and for segment b the cross-correlation shows strong positive correlation, and, for segment c and d, the cross-correlations show obviously positive correlation but with a lower correlation coefficients than that of segment b.

These spectra can be fitted by the multi-color disk model (*diskbb* in XSPEC) plus black body (*bbody* in XSPEC) (e.g., Weng & Zhang 2011). A gaussian line with the center energy fixed at 6.6 keV and the width fixed at 0.5 keV is added to describe the iron line. The photo-electric absorption is modelled with *wabs* in XSPEC. Due to the absence of low energy observation of PCA, the absorption column is fixed at the value of $N_{\rm H} = 3.4 \times 10^{21}$ cm^{-2} (Christian & Swank 1997).

Figure 3 and Table 3 show the fitting results, from segment a to d, as the X-ray flux decreasing, both the disk temperature and black body temperature decrease independently. We can see that, with the increasing of the flux (from d to a), the inner disk radius($\propto$ the normalization) decreases, as the region of black body emission ($\propto$ the normalization) increases. In addition, for segments a and d, both the soft and hard components dominate with the similar weights, the spectral property of which is corresponding to the SPL states of BHXBs (also see Weng & Zhang 2011). For segments b and c, the soft components dominate

the spectral characteristic, which is similar to the HSS of BHXBs (also see Sriram et al. 2010; Weng & Zhang 2011).

4. Summary and Discussion

We have detected the anti-correlation between soft (2-3.3 keV) and hard (12-30 keV) X-rays from the atoll source 4U 1735-44 in 12 *RXTE* observations. The results show that, the observations with anti-correlation are located at the UB, and the observations with positive correlation mostly appear in the LLB and LB. Most observations in the IS show the ambiguous correlation. The pivoting of the wide-band X-ray spectrum is also detected in all the observations with the anti-correlation detected. The energies of pivoting are generally lower than those detected in Z sources, and are not related to their location of CCD (see Table 1).

The results from the atoll source 4U 1735-44 are different from those of Z sources (Lei et al. 2008; Sriram et al. 2012). Most of the anti-correlated observations of Z sources locate at HB and upper NB, which correspond to "the low-hard state", however the anti-correlated observations detected in the atoll source 4U 1735-44 locate at UB which corresponds to high luminosity state. The anti-correlated time lag scales of Z and atoll sources are similar, and the observations with anti-correlated hard X-ray lags are more than those of soft X-ray lags for both Z and atoll sources. For Z source, if the accretion rate is the primary parameter to determine the location on CCD, the anti-correlation could be corresponding to the lower mass accretion. However, the mass accretion rate may be constant for XTE J1701-462 during the Z-track (Lin et al. 2009). Similar to Z sources, there is no obvious relation between the observed delays and corresponding positions on CCD for the atoll source 4U 1735-44.

The anti-correlations have been detected in a few BHXBs with a few hundred to thousand seconds lags with the cross-correlation function of soft and hard X-rays, which suggests that the accretion disk could be truncated (Choudhury et al. 2005; Sriram et al. 2007, 2009, 2010). For two Z sources, Cyg X-2 and GX 5-1, the anti-correlation between soft and hard X-rays favors the truncated accretion disk geometry (Lei et al. 2008; Sriram et al. 2012). The truncated accretion disk model is often used to explain the spectral and temporal features of the hard states observed in BHXBs (Done et al. 2007), however some observational results show that the disk may not be truncated (Miller et al. 2006; Rykoff et al. 2007). The iron line is corresponding to the innermost disk regions (Stella 1990). Done & Gierliński (2006) suggest that truncated disk models are consistent with the detected smeared iron emission line. Done & Diaz Trigo (2010) show that the iron line is instead narrow and consistent with

the truncated disk geometry in GX 339-4. For the atoll source 4U 1705-44, the similar profile of iron emission line is found in the high/soft states, which suggests that the accretion disk could be also truncated in the high/soft states of atoll source (di Salvo et al. 2009). The anti-correlation detected in the high luminosity state should also imply that the truncated disk occurs there.

For BHXBs, Esin et al. (1997) propose that an accretion flow around a BH consists of two zones with a transition radius, an inner advection-dominated accretion flow (ADAF) and an outer standard thin disk. In generally, in the LH state the disk is assumed to be truncated at a large radial distance, and in the HS state it becomes non-truncated. Another suggestion is that the accretion disk is truncated very close to the black hole in the IM state/SPL state from the spectral and temporal results of the study of various black hole sources (e.g, Sriram et al. 2010). The anti-correlation detected in the BHXBs implies that the ADAF condenses and expanses to the inner disk, and therefore the hard X-ray flux increases and soft X-ray flux decreases. The IM state is probably the spectral state where the condensation of the inner hot matter can transform into an inner disk (Liu et al. 2007b; Meyer et al. 2007; Sriram et al. 2010).

The NS has a solid surface and magnetic field, which is different from those of BH. However, if the luminosity of NS LMXB increases above a critical luminosity, its magnetosphere may go inside ISCO, which may account for the same disk evolutionary pattern for BHXBs Weng & Zhang (2011). Our results show that the anti-correlation is detected in the UB which is corresponding to the max flux for the atoll source 4U 1735-44. According to the fitting results of spectra and X-ray luminosity, the LB could be corresponding to the HSS of black hole, and the UB is in accordance with the VHS. Although the different luminosity for IMS and VHS of BHXBs, both states share the similar spectral and timing behavior, and they are often thought as the same state and stand for the transitions between LHS and HSS (Done et al. 2007). The anti-correlations occur at SPL of BHXBs and at UB of NS system (atoll), so we can take the UB of atoll to be similar to SPL of BH system.

Furthermore, we notice that the soft and hard X-rays are not correlated in the IS state for atoll source, which could be due to the fact that the accretion disk boundary is far away from the hot corona where emits the high energy photons. With the accretion rate increasing, the accretion disk moves inward with more soft seed photons produced, at the same time, the ADAF becomes be condensed and produces more hard photons, therefore the positive-correlation occurs, implying the increases of both the soft and hard X-rays. When the luminosity increases above a critical luminosity, the ADAF extends outside to the form of the corona, which expands quickly, so the soft X-rays decrease with the hard X-rays increasing. In the UB, the accretion disk extends down to ISCO and could be truncated

there, and the anti-correlations can be detected. Our spectral analysis suggests that with the increasing of the accretion rate, the inner radius of the accretion disk decreases, which is consistent with BHXBs that the accretion disk could be truncated very close to the compact object (Sriram et al. 2010).

The anti-correlated lags are detected and range from a few tens to hundred seconds in atoll source 4U 1735-44, which are similar to those found in Z sources (Lei et al. 2008; Sriram et al. 2012), but time lags are lower than those in BHXBs (e.g., Choudhury & Rao 2004; Sriram et al. 2009). Generally, the hard X-ray emission could come from the Comptonizing of the soft seed photons. For BHXBs, the soft seed photons could only come from the accretion disk. For NS LMXB systems, the soft seed photons could be produced from the surface of NS and/or the accretion disk. The Comptonizing might occur at a hot corona, a hot flared inner disk, or even the boundary layer between the NS and accretion disk (also see Popham & Sunyaev 2001; Qu et al. 2001). The time scale of only Comptonization process is expected to be about $\lesssim 1$ second, therefore the observed several hundred-second lags could be the other processes(Hasinger 1987; Nowak et al. 1999; Böttcher & Liang 1999). We infer that this anti-correlated lag time scale of about several hundred seconds would be related to the change of the disk structure. The different anti-correlated lag timescale implies that the disk inner radius occurs at various locations, which can also affect corona region. Sriram et al. (2012) suggest that the observed lags could be due to the change in the size of the Comptonizing region. Some authors suggest that the lag time of several hundred seconds is comparable to the viscous timescale during which the various physical and radiative processes change (e.g., Choudhury & Rao 2004; Lei et al. 2008; Sriram et al. 2012). However, above model cannot explain the anti-correlated soft X-ray lag, which can be explained that a fluctuation produced from the innermost accretion disk could propagate to the outer accretion disk and affect the soft X-ray emission regions. The fluctuation of accretion disk by the thermally unstable, which moves outward from the inner to outer disk, perturbs the outer material which can produce the soft X-ray lag at a timescale of a few hundred seconds Li et al. (2007).

I would like to thank the referee. This research has made use of data obtained through the high-energy Astrophysics Science Archive Research Center Online Service, provided by the NASA/Goddard Space Flight Center. We acknowledge the RXTE data teams at NASA/GSFC for their help. This work is subsidized by the Special Funds for Major State Basic Research Projects and by the Natural Science Foundation of China for supports with numbers 2012CB821800 and 2009CB824800 and NSFC numbers 10903005, 11173034, 11173024 and 10903007.

REFERENCES

Altamirano, D., van der Klis, M., Méndez, M., et al. 2008, ApJ, 685, 436

Belloni, T. M. 2010, Lecture Notes in Physics, Berlin Springer Verlag, 794, 53

Belloni, T., et al. 2007, MNRAS, 379, 247

Böttcher, M., & Liang, E. P. 1999, ApJ, 511, L37

Casares, J., et al. 2006, MNRAS, 373, 1235

Choudhury, M., & Rao, A. R. 2004, ApJ, 616, L143

Choudhury, M., et al. 2005, ApJ, 631, 1072

Christian, D. J., & Swank, J. H. 1997, ApJS, 109, 177

Corbet, R. H. D., et al. 1986, MNRAS, 222, 15P

di Salvo, T., D'Aí, A., Iaria, R., et al 2009, MNRAS, 398, 2022

di Salvo, T., et al. 2006, ChJAAS, 6, 010000

Done, C., & Gierliński, M. 2006, MNRAS, 367, 659

Done, C., et al. 2007, A&A Rev., 15, 1

Done, C., & Diaz Trigo, M. 2010, MNRAS, 407, 2287

Esin, A. A., et al. 1997, ApJ, 489, 865

Ford, E. C., et al. 1998, ApJ, 508, L155

Ford, E. C., et al. 2000, ApJ, 537, 368

Galloway, D. K., et al. 2008, ApJS, 179, 360

Hasinger, G. 1987, IAU Symp. 125: The Origin and Evolution of Neutron Stars, 125, 333

Hasinger, G., 1990, Reviews of Modern Astronomy, 3, 60

Hasinger, G., & van der Klis, M. 1989, A&A, 225, 79

Hasinger, G., et al. 1990, A&A, 235, 131

Homan, J., et al. 2010, ApJ, 719, 201

Lei, Y.J., et al. 2008, ApJ, 677, 461

Li, S.L., et al. 2007, ApJ, 666, 368

Lin, D., et al. 2009, ApJ, 696, 1257

Liu, Q.Z., et al. 2007a, A&A, 469, 807

Liu, B.F., et al. 2007b, ApJ, 671, 695

Meyer, F., Liu, B.F., & Meyer-Hofmeister, E. 2007, A&A, 463, 1

Miller, J. M., et al. 2006, ApJ, 653, 525

Mueck, B., et al. 2011, The X-ray Universe 2011, 255

Nowak, M. A., et al. 1999, ApJ, 517, 355

Ng, C., et al. 2010, A&A, 522, A96

O'Brien, K., et al. 2004, MNRAS, 350, 587

Popham, R., & Sunyaev, R 2001, AIP Conf. Proc. 599: X-ray Astronomy: Stellar Endpoints, AGN, and the Diffuse X-ray Background, 599, 870

Qu, J. L., Yu, W., & Li, T. P. 2001, ApJ, 555, 7

Remillard, R. A. 2005, in AIP Conf. Proc. 797, Interacting Binaries: Accretion, Evolution, and Outcomes, ed. L. Burderi et al. (Melville, NY: AIP),231

Remillard, R. A., & McClintock, J. E. 2006, ARA&A, 44, 49

Rykoff, E.S., et al. 2007, ApJ, 666, 1129

Smale, A. P., et al. 1986, MNRAS, 223, 207

Seon, K.I., et al. 1997, ApJ, 479, 398

Sriram, K., et al. 2007, ApJ, 661, 1055

Sriram, K., et al. 2009, RAA, 9, 901

Sriram, K., et al. 2010, ApJ, 725, 1317

Sriram, K., et al. 2012, ApJS, 200, 16

Stella, L. 1990, Nature, 344, 747

van der Klis, M. 2000, ARA&A, 38, 717

van der Klis, M. 2006, in Compact stellar X-ray sources, W.H.G. Lewin & M. van der Klis (eds.), Cambridge University Press, p. 39

van Straaten, S., van der Klis, M., & Wijnands, R. 2005, ApJ, 619, 455

Weng, S.S., & Zhang, S.N. 2011, ApJ, 739, 42

Wijnands, R., et al. 1998, ApJ, 495, L39

Yu, W., & Dolence, J. 2007, ApJ, 667, 1043

Yu, W., & Yan, Z. 2009, ApJ, 701, 1940

Zhang, C. 2007, Advances in Space Research, 40, 1480

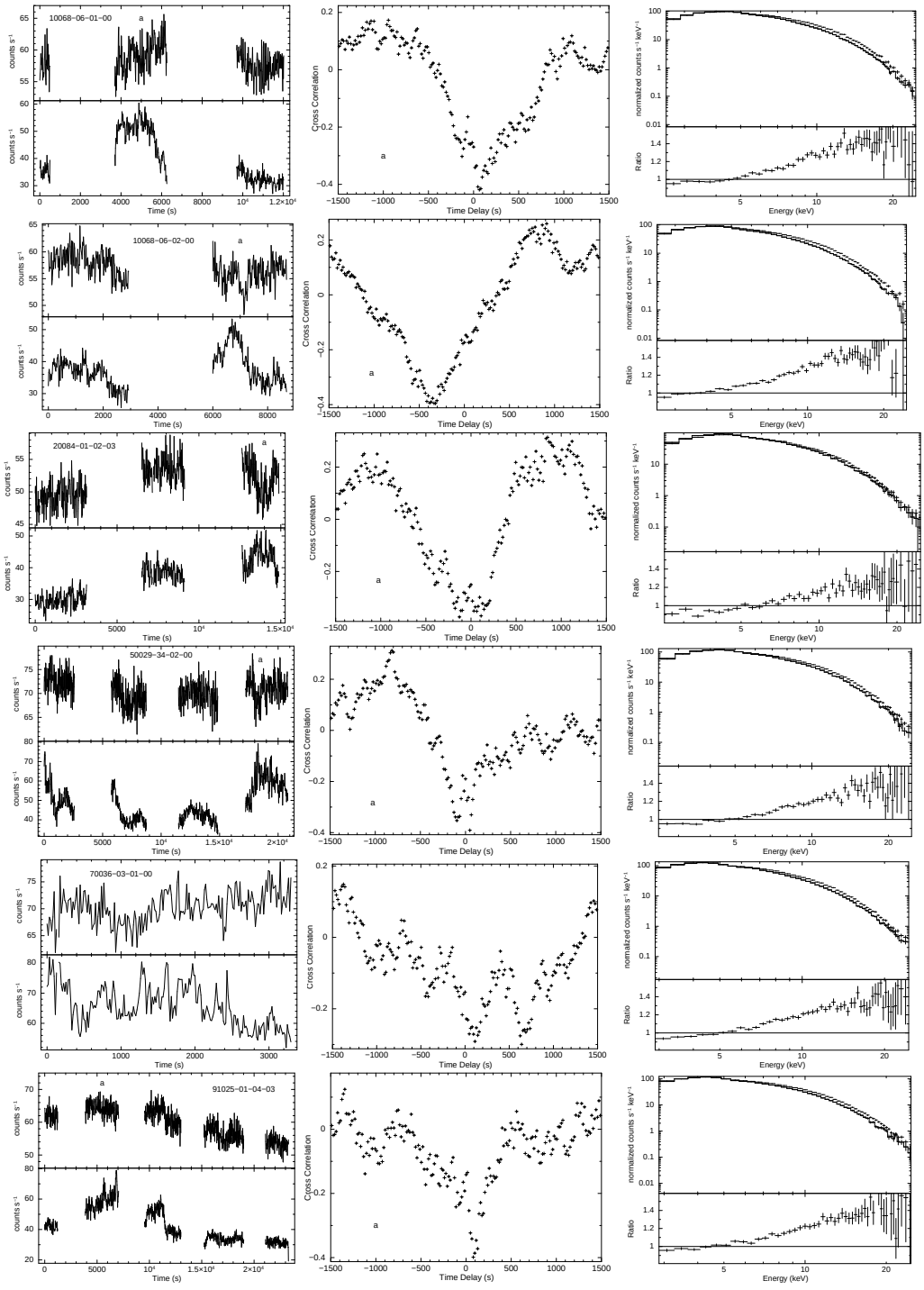

Fig. 1.— The lightcurves (left), cross-correlations between the soft (2-3.3 keV) and hard (12-30 keV) X-rays (middle), the X-ray spectra (right) of the ObsID for hard and soft regions of the light curves are shown.

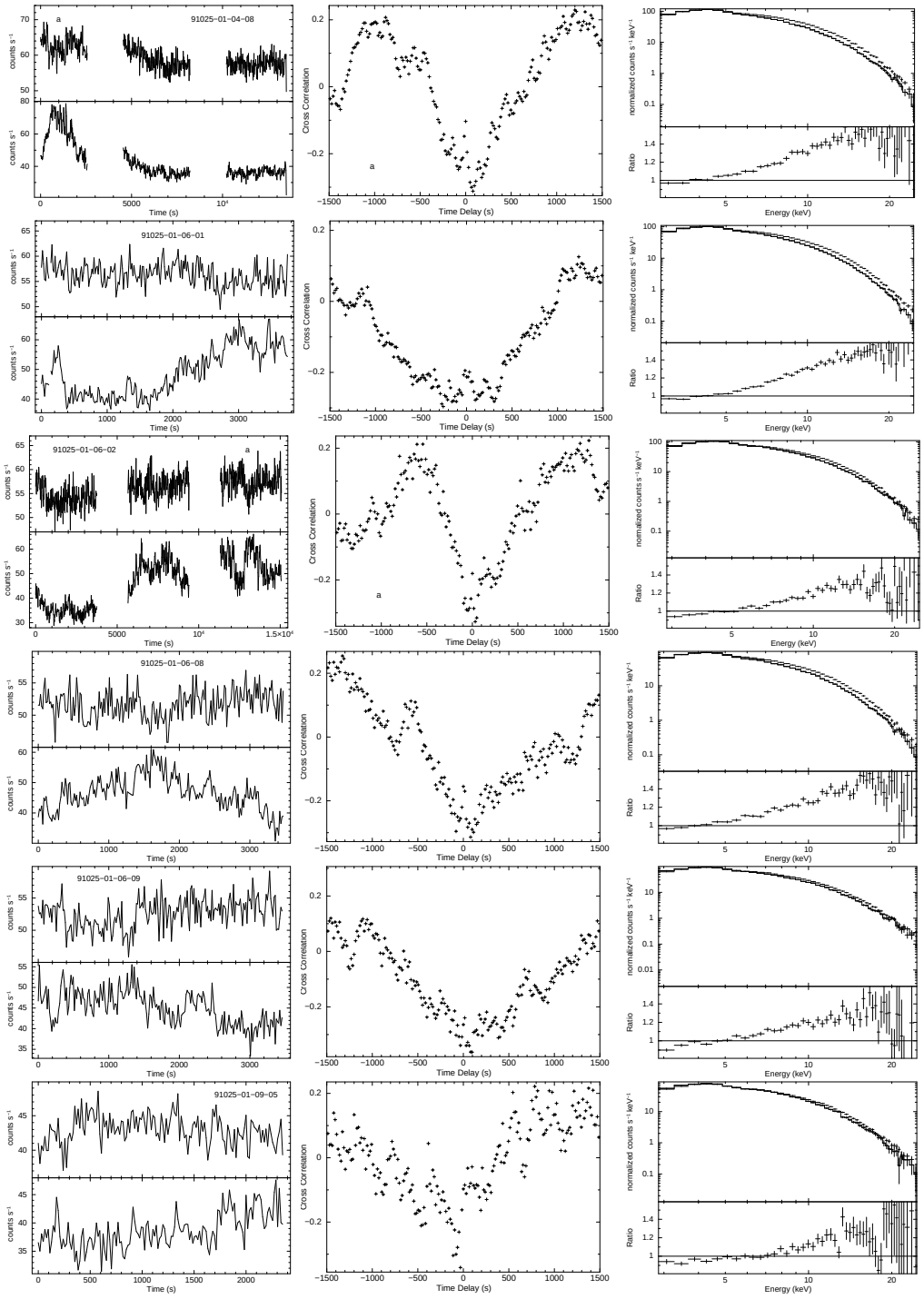

Fig. 1. — Continued.

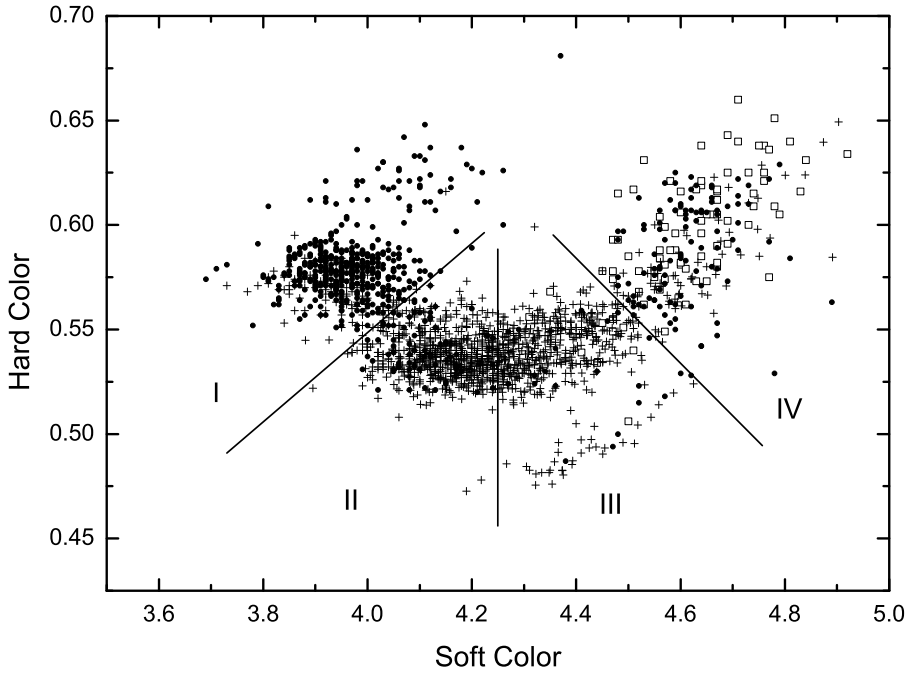

Fig. 2.— CCD of all the analyzed observations is divided into four regions, where squares (dots, crosses) stand for the data with anti-correlation (ambiguous, positive correlation), respectively.

Table 1: **Parameters of ObsIDs where the anti-correlations are detected**

ObsID	Date Year-Month-Day	Location	CC	Delay(Error) (s)	Hardness Ratio	Energy of pivoting (keV)
10068-06-01-00	1996-09-01	III/IV	-0.34±0.02	161±20	4.69/0.60	∼4.5
10068-06-02-00	1996-09-04	III/IV	-0.37±0.01	-350±10	4.562/0.568	∼3.7
20084-01-02-03	1997-09-01	IV	-0.34±0.02	-25.9±24.9	4.636/0.592	∼6
50029-34-02-00	2000-08-14	IV	-0.29±0.03	-16.8±21.0	4.73/0.608	∼5
70036-03-01-00	2002-06-11	IV	-0.20±0.02	317±8	4.827/0.616	∼5.1
91025-01-04-03	2007-01-20	IV	-0.30±0.03	88.7±11	4.665/0.599	∼4.3
91025-01-04-08	2007-01-23	III/IV	-0.27±0.03	63.4±33.4	4.64/0.609	∼4
91025-01-06-01	2007-06-22	III/IV	-0.27±0.04	-113±18	4.571/0.589	∼4.2
91025-01-06-02	2007-06-23	IV	-0.27±0.03	67.6±23.2	4.61/0.607	∼5.1
91025-01-06-08	2007-06-27	III/IV	-0.25±0.02	152±28	4.584/0.601	∼3.9
91025-01-06-09	2007-06-28	III/IV	-0.30±0.02	154±24	4.495/0.593	∼4.7
91025-01-09-05	2008-01-13	IV	-0.18±0.02	-192±49	4.574/0.596	∼7

Table 2: **Percentage of positive and anti-correlation for each region of Fig. 1**

	I	II	III	IV
positive-correlation	19%	90%	94%	28%
anti-correlation	0%	0%	2%	30%
ambiguous	81%	10%	4%	42%

Table 3: **The fitting parameters of the spectra of ObsID 91025-01-04-03**

Parameters	kT_{in}(keV)	N_{disk}	kT_{bb}	N_{bb}	$Flux_{diskbb}/Flux_{total}$	$Flux_{bb}/Flux_{total}$	χ^2(d.o.f)
a	1.95±0.09	18.6±2.8	2.72±0.05	0.051±0.003	4.07/8.23 (49.5%)	4.12/8.23 (50.1%)	1.20(45)
b	1.86±0.07	21.4±2.6	2.68±0.05	0.040±0.002	3.91/7.22 (54.2%)	3.26/7.22 (45.2%)	0.84(45)
c	1.73±0.05	25.7±2.7	2.65±0.04	0.031±0.002	3.32/5.91 (56.2%)	2.55/5.91 (43.1%)	1.20(45)
d	1.63±0.05	39.9±3.6	2.59±0.03	0.031±0.002	2.75/5.51 (49.9%)	2.66/5.51 (48.3%)	1.31(45)

The flux in unit of 10^{-9} ergs cm^{-2} s^{-1} is calculated in the energy band 2-30 keV. Errors are quoted at a 90% confidence level. The letters a, b, c and d stand for the segments in the light curve.

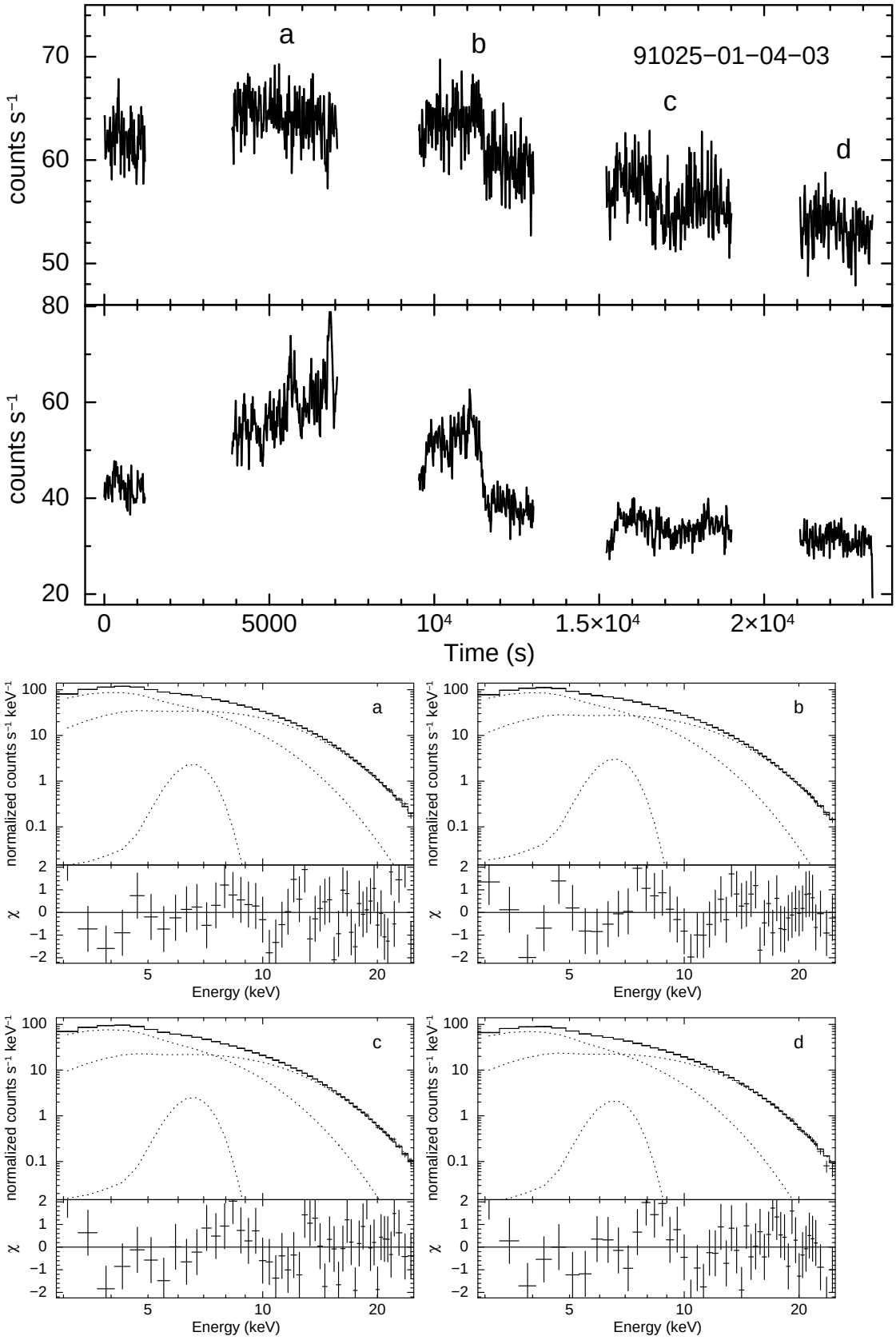

Fig. 3.— Top: The light curves of soft and hard X-rays of ObsID 91025-01-04-03. Middle and Bottom: The unfolded spectrum for each segment is plotted along with its model components.